5 Imaging and Functional Mapping of Local Circuits and Epilepsy

Kenneth M. Little and Michael M. Haglund

CONTENTS

5.1 INTRODUCTION

Optical imaging (OI) is a functional imaging method that measures changes in nervous tissue light reflectance or transmission. OI has been used to study brain functions in both normal and pathophysiological states. In addition to identifying brain function in a way that is not possible with single photon emission computed

tomography (SPECT), positron emission tomography (PET), and functional magnetic resonance imaging (fMRI), OI has provided a greater understanding of the physiologic mechanisms underlying these imaging methods. This chapter will present overviews of different imaging techniques, principles of optical imaging (see Figure 5.1), various studies performed at different levels of brain analysis, and finally, human open optical imaging studies.

5.2 OVERVIEW OF FUNCTIONAL IMAGING TECHNIQUES

Conventional anatomical imaging techniques such as x-ray radiography and computer assisted tomography (CAT) rely upon a photon source that is generated as electrons strike an anode (Bremstrahlung effect). The attenuation of these photons as they pass through tissue and strike silver nitrate film or a fluorescent screen reveals underlying anatomic structures within the interrogated tissue volume. To detect function rather than simply reflecting anatomic structures, functional imaging techniques in general rely upon similar principles and utilize various energy sources and detectors. Functional related changes in nervous tissue trigger water movement into or out of cells or alter the uptake of glucose or other tracers that are indicative of cellular metabolism.

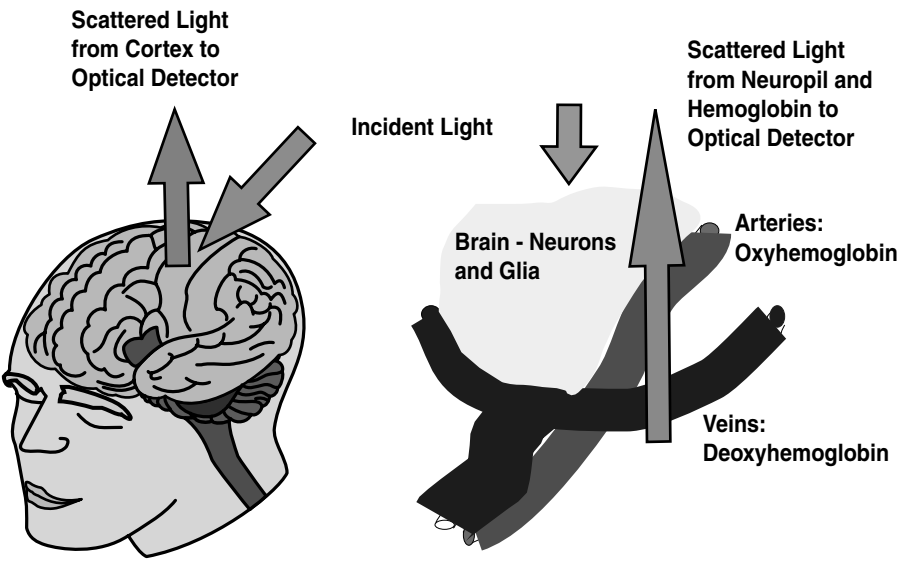

FIGURE 5.1 (See color insert following page 146.) Optical imaging at brain and neuropil levels. Two types of optical imaging approaches: at macro (whole brain) level (left) and at neuropil (micro) level (right). In intact brain, incident light is more or less scattered or absorbed by tissue and its contents, with the resulting scattered light detected by an optical system. At the micro level, scattering occurs in distinct elements that include the neuropil (that has its own intrinsic optical signal), and either oxyhemoglobin or deoxyhemoglobin within the blood vessels. Separate absorption and scattering characteristics appear, depending on the relative content of oxyhemoglobin and deoxyhemoglobin.

5.2.1 Functional MRI

Magnetic resonance imaging (MRI) relies upon an externally generated magnetic field gradient with local radiofrequency-induced disruption. The electromagnetic radiation emitted from the hydrogen dipoles as they reorient from high energy disorganized states to lower energy organized states within the gradient are measured by the detector. Functional MRI (fMRI) uses fast imaging techniques to indirectly detect active neuronal circuits based on relative increases in oxyhemoglobin. This physiological phenomenon results from a local increase in oxygenated blood delivery during neuronal activity. The local increase in oxygenated blood outstrips the generation of deoxyhemoglobin by active tissue, indicating a drop in oxygen extraction by the tissue. The relative decrease in deoxyhemoglobin is detected by blood oxygen level-dependent contrast magnetic resonance imaging (BOLD MRI) "downstream" from the metabolically active tissue.[1] An increasing amount of attention has focused on the initial negative "dip" in the BOLD MRI signal that may indicate transient relative tissue hypoxia before blood flow to the active tissue is increased.

Some studies have compared fMRI directly to cortical electrical stimulation mapping (ESM) performed via open craniotomy or grid stimulation for motor, somatosensory, and language mapping and have demonstrated a correlation between the two methods.[1–7] Significant discrepancies and sources of error, however, mitigate optimistic conclusions that these two modalities are highly correlative. For example, compared to sites identified by ESM, sites of increased activity on fMRI are considerably larger. The radial cortical projections of subsurface fMRI signals used to create functional cortical maps for computer-assisted surgical navigation may not correspond to cortical surface ESM-identified sites.[8] Additionally, due to brain shift during the craniotomy, precise fMRI localization may be prohibitively difficult.

The fMRI areas activated by motor tasks may identify nonessential motor cortex.[9] Differences in language tasks, imaging techniques, data analysis, and brain shift associated with craniotomy have made language mapping particularly difficult to corroborate with ESM results.[4,6,7,10,11] Language tasks that prove to be essential based on intraoperative ESM seem to be best activated on fMRI with semantic decision and verbal fluency tasks; multiple language tasks seem to provide greater sensitivity than any single task.[2,4,10,11] However, limiting fMRI language activation to only essential sites is heavily dependent upon the method of statistical data analysis.[7] According to available evidence, fMRI is subject to errors by (1) identifying areas that are not essential to neurological function, thus potentially limiting the resection unnecessarily; and (2) failing to identify areas that could cause postoperative deficits if resected. In its current state of development, fMRI should be used only as an adjunct to ESM for functional mapping.

Regarding its ability to predict postoperative deficits, one study of sensorimotor cortex in patients undergoing lesion resections demonstrated a correlation between the size of the margin between the lesion (not the resection margin) and area of fMRI activation and the presence of postoperative neurological deficits.[12] However, detailed analysis correlating postoperative deficits to the margin between the *resection cavity* and the area of functional activity is necessary.

Functional MRI has also been used to lateralize language function and several authors have compared fMRI directly to the Wada test (intra-arterial pentobarbital or IAP). Although many studies show promising results, no consensus has yet been reached about which language tasks best correlate with language measures used during IAP or methods of image acquisition and data analysis. Thus, fMRI may be limited in its predictive capability for postoperative deficits.

5.2.2 Positron Emission Tomography

Positron emission tomography (PET) scanning detects photons generated after nuclear decay from the annihilation of positrons with electrons. The photon detectors often consist of bismuth germinate or scintillators coupled to photomultiplier tubes to convert the photons into an electrical signal. PET can be used to detect neuronal activity based on metabolically dependent increased glucose utilization or associated increases in regional cerebral blood flow. The increase in metabolism is detected by fluoro-deoxyglucose (FDG-PET) and blood flow changes are detected by ^{15}O water PET.[13] Due to the limits of radiation dosing, the use of FDG-PET has been limited to mapping primary sensory and motor areas whereas ^{15}O water PET can be infused several times, making it suitable for mapping higher cognitive functions.[13–16]

PET scanning has undergone comparisons to ESM. As with fMRI, studies have shown that compared to essential language sites identified by ESM, sites of language-associated increased PET activity are considerably larger and they may identify language sites where ESM does not disrupt language. The PET-activated sites may be up to 1 cm from the site identified by ESM. Depending upon which tasks are combined to produce activation maps and the method of statistical analysis, PET may fail to identify essential language cortex. Although PET seems inaccurate and unreliable for language localization, it may be adequate for language lateralization. When PET was directly compared to IAP, a study demonstrated a positive predictive value for language lateralization in 80 to 91% of patients, depending on the method of image analysis.[16]

5.2.3 Single Photon Emission Computed Tomography

Single photon emission computed tomography (SPECT) is related to PET but does not require short-lived isotopes. It most often utilizes Technetium-99m (Tc-99m)-labeled pharmaceuticals. The radiolabeled drugs deposit in neural tissue where positrons are emitted. The emitted positrons release photons (gamma rays) as they annihilate with electrons. The gamma rays are detected by a scintillation counter rotating about the patient's head. SPECT scanning has been used to detect pathologic increases and decreases in regional blood flow. Compared to PET, the spatial resolution of SPECT is inferior, but it provides a convenient method of assessing regional cerebral perfusion. This estimate of regional perfusion is highly limited by the large voxel sizes and the static nature of the imaging process, so generally it has been limited to studies of brain death when it is used to detect an absence of cerebral blood flow.

5.2.4 Optical Imaging

Optical imaging (OI) is one of the most recently developed functional mapping techniques for the identification of epileptic foci and eloquent cortical regions.[17–20] Similar to most conventional imaging techniques, OI relies upon photons and their interactions with tissues to measure changes in a tissue's optical scattering and absorption from one physical state to another (see Figure 5.1). Unlike the higher energy photons generated by Bremstrahlung and positron annihilation, the photons used in OI are generated by light within the near-infrared (low frequency) to ultraviolet range, and are therefore of considerably lower energy. They may be captured by various forms of optical detectors and lens systems including a video camera, charge-coupled device (CCD) camera, single photodiode, photodiode array, or the observer's retina.

When the light frequency is changed through filtering, specific physiological properties coupled to neuronal activity can be measured, including regional cerebral blood volume changes at the capillary and venous levels, blood oxygenation changes, cytochrome redox states, and cellular, extracellular, or organelle swelling due to ion gradient changes. These properties can be measured across a broad range of spatial resolution from microscopic neuronal populations to macroscopic cortical regions, depending on the type of microscope and lens system used. In addition to excellent spatial resolution versatility, the temporal resolution is superior to fMRI and PET scanning, making it ideal for imaging epileptiform and functional activity. At near-infrared wavelengths, this technique allows for the added benefit of noninvasive monitoring.[18–21]

5.3 PRINCIPLES OF OPTICAL IMAGING

Optical imaging encompasses several subsets of analysis, including direct reflectance or transmittance imaging (at the same wavelength of light, to detect scattering or absorption), fluorescence imaging, and near-infrared imaging of hemoglobin. Additionally, the scale of analysis varies considerably, from single cell resolution to imaging larger regions of brain for functional activation.

5.3.1 Optical Properties of Neuronal Tissue

Electromagnetic radiation (i.e., photons) interacts with targeted tissue substrates in different ways. The principal interactions between photons and neural tissue relevant to optical imaging are *scattering* and *absorption*.

Scattering: Light scattering in neural tissue is a combination of phenomena. *Rayleigh scattering* is a scattering of light by objects that are small in comparison to the incident light wavelength; the scattering flux density is proportional to the fourth power of the incident light frequency. Thus, high frequency, short wavelength light at the blue end of the visible spectrum is scattered about 10 times more intensely than low frequency, long wavelength light at the red end of the spectrum. This makes near-infrared light more suitable for noninvasive optical imaging through skin and bone, compared to higher frequency light, as less energy is lost to scattering.

When light travels from one medium to another, a portion of the light will be *reflected* away and part will pass through at a *refracted* vector, as described by Snell's law. This submicroscopic process is due to the compositions and densities of scattering molecules at, for example, lipid membrane–cytoplasm interfaces where light reflection and refraction are altered by physiological processes that change the chemical composition or geometry of the interface. Scattering also occurs intracellularly at the organelle/cytoplasm boundaries (mitochondria, nuclei, etc.).

Light may be reflected or refracted from a moving particle (e.g., erythrocytes, albumin) and undergo a *frequency shift* (Doppler shift). By focusing light on blood vessels, Doppler shifts may be used to calculate changes in blood flow. When the incident light is polarized, intracellular, membrane, and extracellular macromolecules may exhibit different refractive indices depending upon the orientation of polarized light. This effect is referred to as *birefringence*. Birefringence can provide information about intermolecular associations within cell membranes and nerve fibers. In an electric field, molecules may become birefringent. This phenomenon, known as the "Kerr effect," can be seen during changes in transmembrane electric potential gradients. For example, axonal membrane molecules with dipole moments can change orientation in a highly ordered fashion during depolarization. This reorientation results in transient birefringence until electric potential gradients are reestablished.

Absorption: Light entering tissue may be either reflected or may pass through after refraction. However, some of the light entering will not pass through the tissue and is therefore said to be *absorbed*. After the energy is transferred to other molecules, the excited recipient molecules eventually return to their more stable ground states. Because energy is conserved, the energy from the absorbed light must be converted and may be dissipated as *fluorescent emission*, *thermal energy*, or *phosphorescence*. For example, the reduced form of nicotinamide adenine dinucleotide (NADH) exhibits intrinsic fluorescence whereas NAD^+ does not. Investigators have taken advantage of this difference to use fluorescence as a sensitive measure of intracellular oxidation states.

In addition to the light scattering and absorption properties intrinsic to neural tissue, photons may interact with a variety of structurally or functionally partitioned dyes to produce phosphorescence or fluorescence. While this can augment imaging based on a tissue's intrinsic optical properties, the advantage of imaging the intrinsic optical signal alone is that it obviates the need for administrating optically active chemicals. A tissue's optical properties in the absence of optical dyes are referred to collectively as intrinsic optical properties. The resulting signal is referred to as the intrinsic optical signal (IOS).

5.3.2 Physiologic Processes Underlying the Intrinsic Optical Signal

Several physiologic processes have been shown to alter the intrinsic optical properties of neural tissue and may be divided into *blood-independent* and *blood-dependent* events or processes.

Blood-independent processes: A blood-independent IOS is generated primarily by cellular processes (the interface between outer membrane and extracellular space) and intracellular interfaces. Cellular events contributing to the IOS have been investigated in neurons and axons in isolation and in brain slices, free from the influences of blood volume and blood oxygenation changes.[22,23] Evidence suggests that neurons and their subcellular organelles including the nuclei and mitochondria swell to varying degrees at different levels of brain activity or injury.[23]

Cellular and organelle swelling in response to transmembrane ion gradient changes may lead to intrinsic optical changes in more than one way. A decrease in the concentration of light-scattering particles results in decreased light scattering and increased light transmittance. Changes in the cellular membrane geometries during swelling lead to changes in light reflectance relative to the angle of the recording device (i.e., CCD camera). Finally, changes in the refractive indices across the membranes that accompany changes in concentration gradients lead to changes in light refraction. Non-neuronal cells in brain tissue also show IOS changes. For example, MacVicar et al. (2002) demonstrated that IOS changes in glia during stimulation are also in part explained by NA/K-2CL cotransporter-induced astrocyte swelling.[24]

Intracellular events other than those attributable to volume changes also contribute to the IOS. Cytochrome C oxidase (Cyt-Ox) is the terminal electron acceptor of the mitochondrial electron transport chain and the energy generated in this process is used to synthesize adenosine triphosphate (ATP). Early studies of Cyt-Ox and NADH redox states in isolated mitochondria demonstrated transient oxidation during increased cellular activity.[25] Using a modified Lambert–Beer law, the light absorption changes accompanying changing Cyt-Ox redox states may be used *in vitro and in vivo* to measure transient cellular energy metabolism changes associated with brain activity.[26]

Blood-dependent processes: Optical imaging *in vivo* adds the additional dimension of vascular changes, making the interpretation of IOS changes more complex. Frostig et al. postulated that activity-related vascular IOS changes represent changes in blood oxygenation and volume.[27] Similar to Cyt-Ox, oxygenated hemoglobin (Oxy-Hb) and deoxygenated hemoglobin (Deoxy-Hb) have characteristic absorption spectra and, based on a modified Lambert–Beer law, changes in their concentrations contribute to the IOS. Blood volume changes have been postulated as contributing to the IOS in that changes in total hemoglobin (Oxy-Hb + Deoxy-Hb) reflect changes in corpuscular blood volume.[27,28]

Finally, changes in a tissue's optical parameters occur with differing latencies. A fast component (onset of 2 to 3 seconds) correlates with neuronal membrane electrical potential changes and a slower component (onset of 3 to 6 seconds and resolving about 20 seconds after the stimulus is removed) that may be associated with cellular and organelle volume changes.[28]

5.4 OPTICAL IMAGING METHODS

Since their initial use by Hill and Keynes, several investigators have developed OI methods for *in vitro* and *in vivo* animal models. Over the past decades, further

technical advances have led to OI use in humans. Current methods include specific techniques for brain slices, open cortical mapping, stereotactic surgery, and transcranial imaging. The following is a brief overview.

5.4.1 Brain Slices

Lipton was the first to investigate the effects of membrane depolarization on light scattering in cerebral cortex slices.[29] Lipton observed that optical reflectance increased when the superfusate osmolarity was increased, and reflectance decreased when the osmolarity decreased below baseline conditions. Assuming that cell volumes increase with decreasing extracellular osmolarity, it was concluded that cell volume changes were inversely related to reflectance changes. Electrical stimulation across the tissue or exposure to high potassium concentrations caused decreases in reflectance, indicating that stimulation also led to increases in cell volumes.

MacVicar and Hochman were the first to apply digital imaging methods to obtain high-resolution synaptic-evoked changes in light transmission through hippocampal brain slices.[30] Specifically, pyramidal CA1 neurons were imaged concurrently with microelectrode recordings during Schaffer collateral bipolar stimulation in the CA3 region. The authors used this method to conduct a sequence of experiments designed to determine the physiological mechanisms underlying optical changes. Aitken et al.[31] identified four subtypes of physiologic processes leading to IOS responses consisting of:

1. Synaptic activation
2. Hypoxia
3. Spreading depression in the presence of normoxia or hypoxia
4. Extracellular osmolarity changes

In addition to studying normal physiology, brain slice OI holds promise in uncovering mechanisms underlying epileptiform activity. Hochman et al. demonstrated that optical changes are associated with epileptiform burst discharges.[32] Using furosemide, the authors were able to block the optical changes and epileptiform activity without blocking synaptic transmission or reducing the hyperexcitable response to electrical stimulation. It may be inferred that optical changes are more closely related to epileptiform activity through synaptic hypersynchronization, rather than hyperexcitability. Also, the intrinsic optical signal changes seen in brain slice preparations may reflect mechanisms critical for the generation of synchronized activity (i.e., seizure activity). This last hypothesis suggests the possibility of applying brain slice OI to screening anti-epileptic drugs.[19]

5.4.2 Open Brain Mapping

The open OI mapping technique became feasible when Blasdel and Salama employed a television camera (120×120) to improve the spatial resolution previously achieved with standard photodiode arrays (12×12).[33] Blasdel went on to apply OI for *in vivo* functional mapping by augmenting the IOS with voltage-sensitive

dyes to image ocular dominance columns and orientation preferences in nonhuman primate visual cortex. Grinvald, Frostig, Ts'o, Lieke, and colleagues were later able to identify similar functional regions in primate visual cortex without using voltage-sensitive dyes by directly imaging the IOS changes associated with cortical surface optical reflectance.[27,34–36] Haglund and colleagues were the first to employ OI intraoperatively in humans. They obtained OI maps of somatosensory, motor, and language cortex in patients undergoing awake craniotomies for intractable epilepsy.[37] Subsequently, Haglund and a handful of investigators employed OI to study sensorimotor,[37–40] language,[37,41,42] and cortical regions subserving higher cognitive functions such as face matching and short-term memory.[40]

Optical imaging represents a significant breakthrough for the study of functional and epileptiform cortical activation. The author's current intraoperative setup allows investigation of microscopic neuronal populations with a spatial resolution of about 60 μm to cortical regions as large as 5×5 cm. We image with a temporal resolution of 200 milliseconds. These benefits allow greater accuracy in intraoperatively delineating Rolandic and language cortex, identifying interictal epileptiform discharges, pinpointing the onsets of ictal events with precise localization, and directly observing the pathways by which seizure activity spreads. Because OI relies upon physiological cortical activation rather than direct stimulation from external electrical currents, it can facilitate and enhance the intraoperative identification of cortical regions subserving cognitive functions.

Several sources of artifacts can make the IOS difficult to discern; successful intraoperative OI requires minimizing patient movement, dampening physiologic brain pulsations, and uniform cortical surface illumination. One of the most critical strategies during OI is to minimize movement. Brain pulsations associated with hemodynamic and respiratory patterns cause spatial shifts during image acquisition making frame-to-frame IOS analysis difficult.[38] This artifact can be overcome during image acquisition with mechanical dampening and during image analysis with image "warping" algorithms. Mechanical dampening is achieved by placing a glass plate (4, 9, 16, or 25 cm^2) over the cortical surface in the area of interest. The glass plate is mounted to an adjustable mechanical arm mounted to a skull clamp. This rigid construct has become particularly important during awake craniotomies and during imaging of seizure activity when image acquisition is continuous over 1 or 2 minutes.

The brain surface is uniformly illuminated using a stable tungsten halogen light source. The incident light is filtered to the desired wavelength (typically using a 695-nm long-pass filter) with the operating theater darkened to minimize artifacts from ambient light sources. By selecting different wavelengths of light through filtering, differential aspects of the IOS, and therefore specific physiological processes, may be emphasized. For example, imaging through a 610- or 695-nm filter, as reported in human studies, emphasizes changes in hemoglobin oxygenation.[38,39,41–43]

A CCD camera is mounted on the operating microscope. To further minimize movement artifacts, the microscope is mounted to the operating table by a modified microscope base. Initially, a low-power objective is selected to allow for visualization of a relatively large cortical area (25 cm^2). During seizure focus localization or

functional mapping, images are collected at a rate of about 50 Hz over a period of 1 minute. Using software developed by Daryl Hochman, image analysis can then be performed intraoperatively within 2 minutes.

Images are analyzed by subtracting a baseline image (i.e., prior to cortical activation) from all subsequent images, yielding data that reflects changes in the IOS from baseline. During analysis, statistical algorithms are applied to align successive images in order to compensate for residual microscopic movement artifacts. This is particularly important when images are acquired through a high-power objective where small movements are magnified. Each series is viewed intraoperatively to evaluate epileptiform or functional activity. Despite efforts to minimize movement, ambient light, and thermal artifacts, a small amount of noise in the processed images is difficult to avoid. While open OI has been successfully performed in humans, it remains a research tool and will require further reliability testing and technical modifications before it can become feasible for routine clinical use.

5.4.3 Stereotactic Approaches

In 2000, Giller et al. introduced an optical imaging method to aid the identification of border zones between deep nuclei and their surrounding white matter tracts during stereotactic pallidotomy, thalamotomy, and placement of deep brain stimulators.[44] The stereotactically implanted fiberoptic probe consisted of a central light-delivering fiber (tungsten light source) surrounded by six light returning fibers. Light emitted from the probe was scattered by the surrounding brain tissue (target tissue morphology and volume estimated as a ¼ sphere with a 100-micrometer diameter) and delivered to a spectrometer through the six light detecting fibers.

Their earlier investigations utilized light in the near-infrared range between 500 and 1000 nm. The range was later changed to 350 to 850 nm to match hemoglobin's absorption peaks.[45] With each incremental (1 mm) advance of the probe, reflectance was recorded and plotted with respect to wavelength. The normalized data obtained from each resulting graph were validated using postoperative MRI or CT scans merged with preoperative MRIs to assess the probe's trajectory and the structures it passed through at each depth.

The measured slopes obtained from reflectance wavelength plots were significantly greater in white matter (mean of 2.5) compared to those of gray matter (mean of 0.82). The authors demonstrated that stereotactic near-infrared imaging could detect subcortical white matter–gray matter interfaces during stereotactic localization of deep brain nuclei. This may prove a reliable and technically simple alternative to currently used localization methods, including microelectrode recording.

Optical coherence tomography (OCT) was developed to provide high-resolution tomographic images of the retina and anterior eye.[46] This technique has been used in combination with endovascular catheters and endoscopes to image internal organ systems, including cardiac vessel lumina, gastrointestinal lumina, and genitourinary lumina. In principle, it is similar to Giller's fiberoptic probe, with the exception that the tip of the probe rotates at various frequencies through 360 degrees to provide a cross-sectional view. More recently, its utility in detecting functional activity by

measuring light scattering changes during propagation of action potentials has been demonstrated in the sea slug abdominal ganglion. With stereotactic techniques, it may be possible to adapt OCT to study functional activity in deep brain nuclei.

5.4.4 Transcranial Techniques

Near-infrared spectroscopy (NIRS) provides a less invasive alternative to the optical imaging methods described earlier. In 1977, Jöbsis was the first to demonstrate the feasibility of transcranial cortical tissue spectroscopy.[47] Unlike open optical imaging that detects light absorption and scattering changes, NIRS makes the assumption that light scattering is relatively constant and therefore relies on light absorption changes within a range of 650 to 950 nm. Most currently used NIRS systems monitor absorption changes associated with changing hemoglobin oxygenation states during cortical stimulation.[28,48]

Two wavelengths of light are used to differentiate changes in Oxy-Hb and Deoxy-Hb. Most imaging systems consist of 20 to 30 source-detector pairs. Since each detector may receive light from multiple sources, light sources are either sequentially switched on and off at high frequency or the incident light from each source is frequency encoded. Each source-detector pair defines a pixel and, through interpolation algorithms, the pixels are smoothed to form a coarse image. To date, most NIRS studies have involved cognitive tasks including different language paradigms. NIRS studies of primary motor, somatosensory, and visual areas have shown that the technique is a feasible alternative to invasive open imaging and other functional imaging techniques. Seizure activity has also been investigated with the NIRS technique in comparison to SPECT/EEG localization and magnetic encephalography (MEG) focus.

5.5 RESULTS OF OPEN HUMAN OPTICAL IMAGING STUDIES

5.5.1 Somatosensory Cortex

The ability to map somatosensory, motor, and language cortex using OI was first demonstrated by Haglund et al. in patients undergoing awake craniotomies for intractable epilepsy.[37] Initially, tongue and palate sensory areas were identified with intraoperative ESM by evoking subjective tingling in those areas. Patients were then instructed to move their tongues from side to side within their closed mouths. During three trials with OI, tongue movements produced the greatest IOS changes within the tongue and palate somatosensory areas as identified by ESM. These IOS changes were similar to those associated with cortical activation after bipolar stimulation, indicating that they reflected somatosensory cortical activation most likely from sensory feedback associated with tongue movements. Motor cortex associated with face movements (as identified by ESM) demonstrated IOS changes in the negative direction during tongue movement. Similar shifts in the IOS of motor cortex were observed during overt speech.[40]

It is tempting to suggest that these negative IOS changes represent decreased neuronal activity in face primary motor cortex during these simple movements. An alternative explanation is that the increased blood flow associated with somatosensory activation caused a shunting of blood flow away from primary motor cortex. We are currently investigating the relationship of blood volume and electrophysiological changes to determine which mechanism underlies this phenomenon.

Others have corroborated the IOS changes observed with somatosensory activation.[38,39] Cannestra et al. elicited somatosensory cortical activation with median nerve transcutaneous stimulation or 110-Hz finger vibration.[39] A close spatial correlation between cortical evoked potentials and IOS changes was noted. Similarly, Shoham and Grinvald elicited somatosensory cortical activation with electrical and tactile peripheral stimulation in 15 patients undergoing brain tumor or AVM resections under general anesthesia.[38] Optical imaging was accompanied by surface evoked potential recording. Due to the presence of optical signal artifacts, they were unable to draw definitive conclusions. However, they were able to obtain reproducible high-resolution somatosensory IOS maps from the hand area in nonhuman primates. The observed IOS changes associated with peripheral tactile stimulation correlated closely with single and multiunit cortical recordings. These findings confirmed the association of positive IOS changes and somatosensory cortical activation.

5.5.2 Language Cortex

Intraoperative ESM under local anesthesia during object naming is a safe, effective way to identify essential language cortex, particularly with the use of modern intravenous propofol anesthesia and local scalp anesthetic block.[49] Stimulation mapping using other, infrequently tested language-related measures such as naming in another language (including American Sign Language), sentence reading, or recent verbal memory have demonstrated dissociation in their cortical representation[50–52] and, under some circumstances, localizing and sparing these other language-related sites are important in avoiding postoperative deficits.[52]

However, mapping many different language functions, particularly when recent memory is included, is quite lengthy. Intraoperative OI may provide greater efficiency and detail during the functional localization of multiple cognitive and language functions.[37,40–42,53]

Haglund et al. performed OI in the inferior frontal language area (Broca's area) and somatosensory cortex of patients undergoing dominant hemisphere temporal lobe resections under local anesthesia.[37] Optical imaging was performed while patients silently viewed blank slides and named objects displayed on slides presented every 2 seconds.

Images obtained during naming showed activation of the premotor cortex, while the sites identified with ESM as demonstrating speech arrest and palate tingling yielded IOS changes in the opposite direction. The area that showed the greatest positive IOS changes during tongue movement was clearly different from the active area in the naming exercise. The premotor cortical areas from which IOS changes occurred during the naming exercise were similar to those identified on PET images obtained during single-word processing studies.[54,55] The IOS changes were greatest in the anatomical area of cortex classically defined as Broca's area (posterior portion

of the inferior frontal gyrus) and not as expected in areas where electrical stimulation caused speech arrest.

Further topographical definition of Broca's area was demonstrated by Cannestra et al.[44] Broca's area was defined by ESM in five patients undergoing craniotomy under local anesthesia for the resection of brain tumors and vascular malformations. After identification of Broca's area, OI was performed during object naming (n = 5), word discrimination (n = 4), auditory responsive naming (n = 4), and orofacial movement (n = 3) tasks. Two distinct subregions (anterior and posterior) within Broca's area were identified. Both auditory and visual object naming paradigms were associated with increased IOS changes in both the anterior and posterior Broca's subregions. In contrast, word discrimination produced IOS changes only in the posterior subregion.

The authors concluded that this functional heterogeneity may represent subspecialized cortical networks within Broca's area, with anterior regions subserving semantic functions and posterior regions subserving phonological functions. Similar to the findings of Haglund et al., they noted incomplete agreement between ESM identified language sites and IOS changes because ESM and IOS changes overlapped only in the posterior subregion of the OI defined Broca's area.[37]

Optical imaging of posterior, peri-sylvian essential language sites (i.e., Wernicke's area) demonstrated findings similar to those in Broca's area. Haglund et al. demonstrated that in posterior temporal cortex, IOS changes during object naming originated from the general region where ESM elicited naming errors.[37] Similar to findings in Broca's area, the IOS changes covered a somewhat wider surrounding area compared to essential areas identified during ESM localization. All IOS changes were observed in areas near sites where ESM altered naming. The IOS changes appeared within 2 to 5 seconds of initiating naming and disappeared over a slightly longer time following the termination of naming.

Cannestra et al. demonstrated similar findings among six patients undergoing awake craniotomies for tumor or vascular lesion resection.[41] IOS changes were observed from all ESM-defined peri-sylvian language areas and from adjacent cortex. As in Broca's area, they were able to identify subregions subserving different functions. Object naming (n = 6) activated the central and anterior–inferior Wernicke subregions; whereas word discrimination (n = 5) preferentially activated the central and superior subregions. Auditory-responsive naming preferentially activated the central, anterior–inferior, and superior regions. Additional task-specific activations were observed in the inferior–posterior subregion.

Optical imaging of inferior frontal and posterior peri-sylvian language areas has consistently shown that IOS changes are more diffuse than ESM-identified regions. Cannestra et al. demonstrated that these surrounding regions may represent task-specific subregions.[41] This more diffuse cortical language representation identified by optical imaging may account for the occurrence of deficits following resection of cortex within 1 cm of ESM-identified essential language sites.[56] In one case, the temporal resection was performed very close to an ESM-identified posterior temporal essential language site while testing language, and stopped when naming errors occurred. As often occurs under similar circumstances, the patient's language returned to baseline soon after surgery. Interestingly, the resection extended to the

margin of the region of IOS changes, suggesting that OI can provide the reliable localizing information needed to plan safe cortical resections.

5.5.3 Cognitive Function

In more than 20 patients undergoing temporal lobe resections for intractable epilepsy, we studied dominant and nondominant temporal lobe neocortical IOS activation associated with several cognitive tasks.[40] During dominant hemisphere resections, we found that IOS changes associated with short-term memory tasks localized to the posterior–superior temporal gyrus (STG). In these patients, IOS changes associated with object naming overlapped with ESM identified essential language sites.

IOS changes associated specifically with the memory task, however, were immediately anterior to the essential language site. Furthermore, activation with memory input occupied a discrete region that was immediately surrounded by positive IOS changes associated with memory retrieval. In a subset of patients undergoing nondominant hemisphere temporal lobe resections, we performed OI during face matching, complex figure matching, and facial expression interpretation tasks (paradigm described in detail by Ojemann et al).[57] We consistently identified negative IOS changes within the posterior MTG and STG during the tasks.

5.5.4 Epileptiform Activity

Optical imaging can be used intraoperatively to study seizure and interictal activity.[37,58] Prior to imaging, surface EEG is used to roughly localize foci of epileptiform activity. Once localized, the electrocorticogram (ECoG) electrodes are removed from the cortical surface and a glass plate is placed over the site of interest together with an array of recording electrodes about the periphery and a pair of centrally located stimulating electrodes. In addition to imaging spontaneous activity, evoked interictal and seizure activity can be generated through bipolar stimulation at currents above the afterdischarge (AD) potential threshold.

In five patients undergoing surgery for intractable epilepsy, Haglund et al. demonstrated that the IOS intensity, spread, and duration occurring during epileptiform activity evoked from bipolar stimulation correlated with the duration of electrical AD activity.[37] The stimulus was delivered via electrodes separated by 1 cm at an intensity just above the AD potential threshold and the IOS was compared to simultaneous surface EEG recordings. Each stimulation was followed by epileptiform AD activity characterized by varying degrees of intensity and duration.

The spatial spread of the IOS was greatest when associated with long durations of AD activity (12 to 16 seconds) and less when assocaited with short durations of AD activity (<4 seconds). The area of peak IOS intensity during the shorter seizure episode was more limited compared to the much greater spatial extent of IOS changes during the more intense seizure episode. Furthermore, the duration of IOS changes correlated with but lasted longer than the duration of electrical activity. In addition to a greater spatial extent and duration of IOS changes, longer seizure episodes were also associated with a greater magnitude (i.e., greater intensity) of IOS changes. Of interest, but still without a clear mechanism, are the negative IOS changes in the areas surrounding the focus of epileptiform discharges. More detailed studies are

needed to determine whether these negative IOS changes represent surround inhibition, shunting of extracellular fluid, shunting of blood volume toward active cortex, or changes in blood oxygenation.

Further analysis, involving comparisons of IOS changes and surface EEG activity during different stages of seizure activity, reveals that the magnitude and direction of IOS changes appear to correlate with changes in electrical activity. IOS changes and surface electrode activity were measured simultaneously at baseline prior to stimulation, after stimulation during the seizure, during postseizure quiescence, and after return to baseline. During baseline activity, the region surrounding the recording electrode demonstrated neutral IOS whereas during the seizure episode this area was clearly activated in the positive direction. During the postseizure period when the electrical activity was quiescent compared to baseline, the area surrounding the recording electrode showed a negative IOS that gradually returned to near baseline. These preliminary observations pointed toward a correlation between the direction of IOS changes and electrical activity where positive IOS changes closely correlate with increases in electrical activity, and negative IOS changes correlate with below-baseline electrical activity.

5.6 UTILITY OF OPTICAL IMAGING

Optical imaging may become a reliable alternative to conventional mapping techniques (e.g., ESM, fMRI, and PET) and may provide a means to better understand the physiologic processes underlying these techniques. However, it requires full operative exposure of the brain. As described in previous sections, fMRI and PET have not yet proven to be reliable alternatives to ESM. The maps generated by OI, on the other hand, demonstrate better colocalization with ESM-generated functional maps compared to those determined by BOLD contrast.[59] Our initial experiences with OI of language and higher cognitive functions indicate that OI will become a valuable means of mapping and precisely pinpointing cortical representations of higher cognitive processes and assessing the temporo-spatial relationships associated with cortical processing during cognitive tasks. To date, mapping these functions with ESM has been difficult at best and is often limited to functional imaging methods often associated with localization errors.

Noninvasive OI (NIRS) is a promising technique, but several limitations must be overcome. For an excellent review of this subject see Obrig and Villringer.[28] In summary, the authors have identified limited spatial resolution, lack of depth resolution, interference artifacts from extracranial oxygenation changes and systemic hemodynamic changes, and lack of adequate statistical data analysis in the majority of published studies. The stereotactic OI method introduced by Giller et al. may ultimately provide a more convenient alternative to identifying deep nuclear structures based on microelectrode recordings. Optical coherence tomography may provide valuable insights into the functions of deep brain nuclei. However, their routine clinical use will have to await further clinical investigation.

Although OI is not yet ready for routine clinical use, it continues to provide insights into normal and pathological cortical function. Furthermore, it has provided insight into the meaning of fMRI BOLD contrast. For example, OI studies show

that increases in Deoxy-Hb occur within 2 to 3 seconds after stimulus cessation and may represent the initial negative "dip" seen with decreased BOLD contrast during fMRI. Increases in Oxy-Hb are slower and likely correlate with increased BOLD contrast (decreased Deoxy-Hb). The early IOS changes seen with increased Deoxy-Hb (negative BOLD dip) may be temporally and spatially more localizing than the delayed IOS changes corresponding to the increased Oxy-Hb. Evidence suggests that IOS changes associated with increased blood volume in the vicinity of active neuronal tissue correlate well with stimulus-induced activation compared to IOS changes associated with increased Deoxy-Hb and BOLD contrast.

5.7 CONCLUSION

The clinical utility of OI ultimately depends on the continued development of noninvasive approaches, if at all possible, to avoid the current requirement for open brain exposure. As discussed earlier, noninvasive OI techniques have not yet achieved the specificity and reliability of alternative noninvasive techniques and several technical obstacles remain. Early experiences with intraoperative OI, on the other hand, have demonstrated a combination of spatial and temporal resolution that may be optimal for intraoperative functional mapping and seizure focus localization compared to standard techniques.

REFERENCES

1. Mueller, W.M., Yetkin, F.Z., and Haughton, V.M., Functional magnetic resonance imaging of the somatosensory cortex, *Neurosurg. Clin. N. Amer.*, 8, 373–381, 1997.
2. Binder, J., Functional magnetic resonance imaging language mapping, *Neurosurg. Clin. N. Amer.*, 8, 383–392, 1997.
3. Chapman, P.H., Buchbinder, B.R., Cosgrove, G.R., and Jiang, H.J., Functional magnetic resonance imaging for cortical mapping in pediatric neurosurgery, *Pediatr. Neurosurg.,* 23, 122–126, 1995.
4. FitzGerald, D.B. et al., Location of language in the cortex: a comparison between functional MR and electrocortical stimulation, *Am. J. Neuroradiol.,* 18, 1529–1539, 1997.
5. Jack, C.R. et al., Sensory motor cortex: correlation of presurgical mapping with functional MR imaging and invasive cortical mapping, *Radiology*, 190, 85–92, 1994.
6. Rutten, G.J.M., van Rijen, P.C., van Veelen, C.W.M., and Ramsey, N.F., Language area localization with three-dimensional functional magnetic resonance imaging matches intrasulcal electrostimulation in Broca's area, *Ann. Neurol*., 46, 405–408, 1999.
7. Schlosser, M.J. et al., Comparative localization of auditory comprehension by using functional magnetic resonance imaging and cortical stimulation, *J. Neurosurg.,* 91, 626–635, 1999.
8. Krings, T. et al., Functional magnetic resonance imaging and transcranial magnetic stimulation: complementary approaches in the evaluation of cortical motor function, *Neurology*, 48, 1406–1416, 1997.
9. Macdonell, R.A.L. et al., Motor cortex localization using functional MRI and transcranial stimulation, *Neurology*, 53, 1462–1467, 1999.

10. Benson, R.R. et al., Language dominance determined by whole brain functional MRI in patients with brain lesions, *Neurology*, 52, 798–809, 1999.
11. Lehericy, S. et al., Functional MR evaluation of temporal and frontal language dominance compared with the Wada test, *Neurology*, 54, 1625–1633, 2000.
12. Yetkin, F.Z. et al., Functional MR activation correlation with intraoperative cortical mapping, *AJNR*, 18, 1311–1315, 1997.
13. Fox, P.T. et al., Mapping human visual cortex with positron emission tomography, *Nature*, 323, 806–809, 1986.
14. Fox, P.T. et al., Non-oxidative glucose consumption during focal physiological neuronal activity, *Science*, 241, 462–464, 1988.
15. Ginsburg, M. et al., Increases in both cerebral glucose utilization and blood flow during execution of a somatosensory task, *Ann. Neurol*., 23, 152–160, 1988.
16. Hunter, K.E. et al., ^{15}O water positron emission tomography in language localization: a study comparing positron emission tomography visual and computerized region of interest analysis with the Wada test, *Ann. Neurol.,* 45, 662–665, 1999.
17. Gratton, C. et al., Shades of gray matter: noninvasive optical images of human brain responses during visual stimulation, *Psychophysiology*, 32, 505–509, 1995.
18. Hirth, C. et al., Non-invasive functional mapping of the human motor cortex using near-infrared spectroscopy, *Neuroreport*, 7, 1977–1981, 1996.
19. Hochman, D.W., Intrinsic optical changes in neuronal tissue: basic mechanisms, *Neurosurg. Clin. N. Amer.*, 8, 393–412, 1997.
20. Watanabe, E. et al., Noninvasive near infra-red spectroscopic topography in humans, *Neurosci. Lett*., 205, 41–44, 1996.
21. Yamashita, Y. et al., Noninvasive near-infrared topography of human brain activity using intensity modulation spectroscopy, *Optical Eng.*, 35, 1046–1049, 1996.
22. Johnson, L.J., Hanley, D.F., and Thakor, N.V., Optical light scatter imaging of cellular and sub-cellular morphology changes in stressed rat hippocampal slices, *J. Neurosci. Methods,* 98, 21–31, 2000.
23. Fayuk, D., Aitken, P.G., Somjen, G.G., and Turner, D.A., The relationship between extracellular space and intrinsic optical signals in rat hippocampus *in vitro*: synaptic, spreading depression and osmotic-induced signals, *J. Neurophysiol.,* 87, 1924–1937, 2002.
24. MacVicar, B.A., Feighan, D., Brown, A., and Ransom, B., Intrinsic optical signals in the rat optic nerve: role for K(+) uptake via NKCCl and swelling of astrocytes, *Glia*, 37, 114–123, 2002.
25. Chance, B. and Williams, G.R., The respiratory chain and oxidative phosphorylation, *Adv. Enzymol.,* 17, 65–134, 1956.
26. Heekeren, J.R. et al., Noninvasive assessment of changes in cytochrome C oxidase oxidation in human subjects during visual stimulation, *J. Cereb. Blood Flow Metabol*., 19, 592–603, 1999.
27. Frostig, R.D., Lieke, E.E., Ts'o, D.Y., and Grinvald, A., Cortical functional architecture and local coupling between neuronal activity and the microcirculation revealed by *in vivo* high resolution optical imaging of intrinsic signals, *PNAS*, 87, 6082–6086, 1990.
28. Obrig, H. and Villringer, A., Beyond the visible: imaging the human brain with light, *J. Cereb. Blood Flow Metabol*., 23, 1–18, 2003.
29. Lipton, P., Effects of membrane depolarization on light scattering by cerebral cortical slices, *J. Physiol. (Lond.),* 231, 365–383, 1973.
30. MacVicar, B.A. and Hochman, D., Imaging of synaptically evoked intrinsic optical signals in hippocampal slices, *J. Neurosci.,* 11, 1458–1469, 1991.

31. Aitken, P.G., Fayuk, D., Somjen, G.G., and Turner, D.A., Use of intrinsic optical signals to monitor physiological changes in brain tissue slices, *Methods*, 18, 91–103, 1999.
32. Hochman, D.W. et al., Furosemide blockade of epileptiform activity dissociates synchronization from hyperexcitability, *Science*, 270, 99–102, 1995.
33. Blasdel, G.G. and Salama, G., Voltage-sensitive dyes reveal a modular organization in monkey striate cortex, *Nature*, 321, 579–585, 1986.
34. Grinvald, A., Manker, A., and Segal, M., Visualization of the spread of electrical activity in rat hippocampal slices by voltage-sensitive optical probes, *J. Physiol*., 333, 269–291, 1982.
35. Grinvald, A. et al., Functional architecture of cortex revealed by optical imaging of intrinsic signals, *Nature*, 324, 361–364, 1986.
36. Ts'o, D.Y. et al., Functional organization of primate visual cortex revealed by high resolution optical imaging, *Science*, 249, 417–420, 1990.
37. Haglund, M.M., Ojemann, G.A., and Hochman, D.W., Optical imaging of epileptiform and functional activity from human cortex, *Nature*, 358, 668–671, 1992.
38. Shoham, D. and Grinvald, A., The cortical representation of the hand in Macaque and human area S-1: high resolution optical imaging, *J. Neurosci.,* 21, 6820–6835, 2001.
39. Cannestra, A.F. et al., Temporal spatial differences observed by functional MRI and human intraoperative optical imaging, *Cerebral Cortex,* 11, 773–782, 2001.
40. Hochman, D.W., Ojemann, G.A., and Haglund, M.M., Optical imaging reveals alternating positive and negative changes during cognitive or sensory evoked cortical activity in awake humans, *Soc. Neurosci.*, 20, 5, 1994.
41. Cannestra, A.F. et al., Temporal and topographical characterization of language cortices using intraoperative optical intrinsic signals, *Neuroimage*, 12, 41–54, 2000.
42. Pouratian, N. et al., Optical imaging of bilingual cortical representations, *J. Neurosurg.,* 93, 676–681, 2000.
43. Haglund, M.M., Berger, M.S., and Hochman, D.W., Enhanced optical imaging of human gliomas and tumor margins, *Neurosurgery*, 38, 308–316, 1996.
44. Giller, C.A., Johns, M., and Liu, H., Use of an intracranial near-infrared probe for localization during stereotactic surgery for movement disorders: technical note*, J. Neurosurg.,* 93, 498–505, 2000.
45. Johns, M., Giller, C.A., and Liu, H., Computational and *in vivo* investigation of optical reflectance from human brain to assist neurosurgery, *J. Biomed. Optics*, 3, 437–445, 1998.
46. Fujimoto, J.G. et al., New technology for high-speed and high-resolution optical coherence tomography, *Ann. NY Acad. Sci*., 838, 95–107, 1998.
47. Jöbsis, F.F., Noninvasive, infrared monitoring of cerebral and myocardial oxygen sufficiency and circulatory parameters, *Science*, 198, 1264–1267, 1977.
48. Williams, I.M., Mortimer, A.J., and McCollum, C.N., Recent developments in cerebral monitoring: near-infrared light spectroscopy, *Eur. J. Vasc. Endovasc. Surg.*, 12, 263–271, 1996.
49. Silbergeld, D.L. et al., Use of propofol (Diprivan) for awake craniotomies: technical note, *Surg. Neurol.,* 4, 271, 1992.
50. Ojemann, G. and Whitaker, H., Language localization and variability, *Brain Lang.,* 6, 239–260, 1978.
51. Ojemann, G.A., Brain organization for language from the perspective of electrical stimulation mapping, *Behav. Brain Sci.*, 6, 189–206, 1983.

52. Ojemann, G.A. and Dodrill, C.G., Intraoperative techniques for reducing language and memory deficits with left temporal lobectomy, *Adv. Epileptol.*, 16, 327–330, 1987.
53. Cannestra, A.F. et al., The characterization of language cortices utilizing intraoperative optical intrinsic signals, *Neuroimage*, 7, 52, 1998.
54. Petersen, S.E. et al., Positron emission tomographic studies of the cortical anatomy of single word processing, *Nature*, 331, 585–589, 1988.
55. Frith, C.D., Friston, K.J., Liddle, P.F., and Frackowiak, R.S., A PET study of word finding, *J. Neuropsychol.,* 29, 1137–1148, 1991.
56. Haglund, M.M. et al., Cortical localization of temporal lobe language sites in patients with gliomas, *Neurosurgery*, 34, 567–576, 1994.
57. Ojemann, J.G., Ojemann, G.A., and Lettich, E., Neuronal activity related to faces and matching in human right nondominant temporal cortex, *Brain,* 115, 1–13, 1992.
59. Schwartz, T.H. and Bonohoeffer, T., *In vivo* optical imaging of epileptic foci and surround inhibition in ferret cerebral cortex, *Nature Medicine*, 7, 1065–1067, 2001.
59. Pouratian, N. et al., Spatial/temporal correlation of BOLD and optical intrinsic signals in humans, *Magn. Reson. Med.*, 47, 766–776, 2002.